Durham University

Durham Research Online

Deposited in DRO:

29 April 2008

Version of attached file:

Other

Peer-review status of attached file:

Peer-reviewed

Citation for published item:

Angulo, R. and Baugh, C. M. and Frenk, C. S. and Bower, R. G. and Jenkins, A. R. and Morris, S. L. (2005) 'Constraints on the dark energy equation of state from the imprint of baryons on the power spectrum of clusters.', Monthly notices of the Royal Astronomical Society., 362 (1). L25-L29.

Further information on publisher's website:

http://dx.doi.org/10.1111/j.1745-3933.2005.00067.x

Publisher's copyright statement:

The definitive version is available at www.blackwell-synergy.com

Additional information:

Use policy

The full-text may be used and/or reproduced, and given to third parties in any format or medium, without prior permission or charge, for personal research or study, educational, or not-for-profit purposes provided that:

- a full bibliographic reference is made to the original source
- a link is made to the metadata record in DRO
- the full-text is not changed in any way

The full-text must not be sold in any format or medium without the formal permission of the copyright holders.

Please consult the full DRO policy for further details.

Durham University Library, Stockton Road, Durham DH1 3LY, United Kingdom
Tel : +44 (0)191 334 3042 | Fax : +44 (0)191 334 2971
https://dro.dur.ac.uk

Mon. Not. R. Astron. Soc. **000**, 000–000 (0000) Printed 2 February 2008 (MN LATEX style file v2.2)

Constraints on the dark energy equation of state from the imprint of baryons on the power spectrum of clusters.

R. Angulo[1,2], C. M. Baugh[2], C. S. Frenk[2], R. G. Bower[2], A. Jenkins[2], S. L. Morris[2].

[1] *Departamento de Astronomía y Astrofísica, Pontificia Universidad Católica de Chile, V. Mackenna 4860, Santiago 22, Chile.*
[2] *Institute for Computational Cosmology, Department of Physics, University of Durham, South Road, Durham, DH1 3LE, UK.*

arXiv:astro-ph/0504456v2 13 Jun 2005

2 February 2008

ABSTRACT

Acoustic oscillations in the baryon-photon fluid leave a signature in the matter power spectrum. The overall shape of the spectrum and the wavelength of the oscillations depend upon the sound horizon scale at recombination. Using the Λ cold dark matter Hubble Volume simulation, we show that the imprint of baryons is visible in the power spectrum of cluster-mass dark matter haloes, in spite of significant differences between the halo power spectrum and the prediction of linear perturbation theory. A measurement of the sound horizon scale can constrain the dark energy equation of state. We show that a survey of clusters at intermediate redshift ($z \sim 1$), like the Sunyaev-Zeldovich survey proposed by the South Pole Telescope or a red sequence photometric survey with VISTA, could potentially constrain the sound horizon scale to an accuracy of $\sim 2\%$, in turn fixing the ratio of the pressure of the dark energy to its density (w) to better than $\sim 10\%$. Our approach does not require knowledge of the cluster mass, unlike those that depend upon the abundance of clusters.

1 INTRODUCTION

Estimates of cosmological parameters have improved dramatically with the advent of accurate measurements of temperature anisotropies in the microwave background radiation and the clustering of local galaxies (Efstathiou et al. 2002; Percival et al. 2002; Spergel et al. 2003; Abazajian et al. 2004; Tegmark et al. 2004). A consistent picture is emerging, the ΛCDM model, in which the geometry of the Universe is flat (or very nearly so), with matter accounting for less than 30% of the required critical density (de Bernardis et al. 2000; Peacock et al. 2001; Cole et al. 2005). Several lines of evidence indicate that the shortfall in energy density is made up by "dark energy" (Riess et al. 1998; Perlmutter et al. 1999; Efstathiou et al. 2002; Spergel et al 2003).

The dark energy exerts a negative pressure and is responsible for the current acceleration of the expansion of the Universe. The equation of state of the dark energy, the ratio of its pressure to density, is specified by a parameter $w \equiv P/\rho$. For a vacuum energy or cosmological constant, $w = -1$ at all times; in quintessence models, the equation of state can vary with time, i.e. w is a function of redshift (Linder 2003). Theoretically, dark energy is poorly understood and progress will require the design and implementation of new cosmological tests to constrain its properties.

There has been much speculation about using the wavelength of acoustic oscillations imprinted on the galaxy power spectrum to constrain the dark energy equation of state (Blake & Glazebrook 2003, hereafter BG03; Linder 2003; Seo & Eisenstein 2003). This scale depends on the size of the sound horizon at recombination and is the maximum distance that a ripple in the baryon-photon fluid can travel before the sound speed drops precipitously after recombination, stifling any further propagation. The acoustic horizon is a standard ruler that depends only on physical parameters (e.g. the physical densities in matter, $\Omega_m h^2$, and baryons, $\Omega_b h^2$, in units of the critical density; h is the Hubble parameter) and is determined from the acoustic peaks in the cosmic microwave background (Spergel et al. 2003). The observed wavelength of oscillation depends upon the geometry of the Universe and thus on the dark energy equation of state.

Using the "Millennium" N-body simulation of a ΛCDM universe, Springel et al. (2005) demonstrated that acoustic oscillations are visible in the matter power spectrum at the present day, albeit in a modified form. The maximum relative amplitude of the oscillatory features in the matter spectrum is around 10%, much smaller than the acoustic peaks in the power spectrum of the microwave background (Meiskin, White & Peacock 1999). The detection of these features therefore demands precision measurements of large-scale clustering, which is only possible with a survey covering a large volume. The imprint of baryons in the galaxy distribution was detected in the power spectrum of the 2-degree field galaxy redshift survey (Percival et al. 2001; Cole et al. 2005) and the correlation function of luminous red galaxies (Eisenstein et al. 2005). These detections lack the accuracy needed for a competitive estimate of w.

Galaxy clusters are an attractive alternative to galaxies for mapping the large-scale structure of the Universe. Rich clusters are easier to detect at large distances than individual galaxies and their mean separation is much greater. Thus, it is easier to sample large volumes homogeneously with clusters than with galaxies. The low space density of

clusters might appear at first sight to make the power spectrum difficult to measure. However, clusters have a stronger correlation amplitude than the overall mass distribution and this offsets their sparsity (Kaiser 1984; for an illustration of how clustering depends on group size see Padilla et al. 2004).

In this letter, we first show that the imprint of baryons on the matter power spectrum is indeed visible in the power spectrum of galaxy clusters (Section 2). We do this using the "Hubble Volume" N-body simulation of a ΛCDM universe, modelling a range of phenomena that alter the appearance of the oscillatory features in the power spectrum as clustering develops. The power spectrum of clusters is very different from the prediction of linear perturbation theory so our approach represents an improvement over previous studies (e.g. Hu & Haiman 2003; Wang et al. 2004). In Section 3, we assess the accuracy with which the sound horizon scale can potentially be recovered for samples of dark matter haloes that are relevant for forthcoming cluster surveys. The prospects for constraining the dark energy equation of state are discussed in Section 4.

2 THE POWER SPECTRUM OF CLUSTERS

The power spectrum of density fluctuations in the linear regime is a well specified prediction of the cold dark matter model (Bardeen et al. 1986). While fluctuations around the mean density remain small, the evolution of the spectrum can be accurately calculated using linear perturbation theory. In this case, the shape of the spectrum is preserved but its amplitude changes. As the perturbations grow, various processes cause the power spectrum of galaxies or clusters to differ from the linear theory expectation: (i) *Nonlinear evolution.* Mode coupling due to gravitational instability influences fluctuation growth and alters the shape of the power spectrum. (ii) *Biasing between the spatial distribution of mass and its tracers.* In general, the distribution of galaxies or clusters does not constitute a random sampling of the mass and the two could be related in a complicated way (e.g. Bower et al. 1993). In the simplest model, the difference between the clustering amplitudes of the mass and the tracers is described by a bias parameter, which can vary with scale and redshift (e.g. Cole et al. 1998; Narayanan, Berlind & Weinberg 2000). (iii) *Peculiar motions and redshift errors.* The effect of peculiar velocities on measured redshifts is to introduce a redshift-space distortion. On large scales, this takes the form of coherent flows towards massive structures that boost the apparent amplitude of the power spectrum (Kaiser 1987). On small scales, random motions inside virialized objects smear out structures, damping the power spectrum. Errors in the redshift determination also damp the spectrum at intermediate and large wavenumbers but do not boost the spectrum at low wavenumbers.

These effects are best modelled with a N-body simulation of hierarchical clustering. We use the $z = 1$ output of the Virgo Consortium's "Hubble Volume" simulation of a ΛCDM universe (Jenkins et al. 2001; Evrard et al. 2002). This had a volume of $27h^{-3}\mathrm{Gpc}^3$ and a particle mass of $2.2 \times 10^{12} h^{-1} M_\odot$, making it ideally suited to studying the clustering of massive haloes (Colberg et al. 2000; Padilla & Baugh 2002). Dark matter haloes are identified using the friends-of-friends algorithm (Davis et al. 1985).

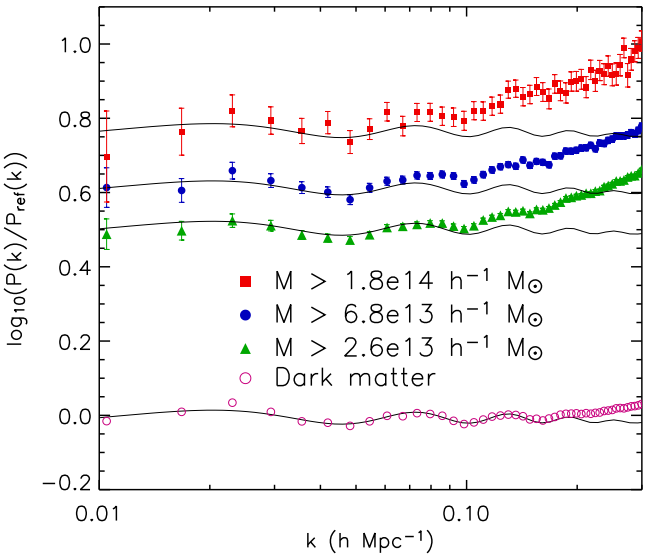

Figure 1. The real-space power spectrum of the dark matter (open circles) and various samples of dark matter haloes (filled symbols). The halo samples are defined by the minimum mass threshold given in the legend. The spectra have all been divided by a reference cold dark matter power spectrum without baryons. The solid lines show the linear perturbation theory prediction, divided by the same reference. For the halo samples, the lines have been multiplied by the square of an effective bias parameter. The error bars are computed using Eq. 1.

Fig. 1 shows the impact on the power spectrum of processes (i) and (ii) above: nonlinear evolution and bias. The open points show the power spectrum of the dark matter at $z = 1$. To expand the dynamic range, the spectrum has been divided by a cold dark matter power spectrum that does not contain any contribution from baryons. The solid line shows the linear perturbation theory spectrum for the simulation parameters, divided by the same reference. The amplitude of spectrum of the dark matter is systematically higher than the linear theory prediction for $k > 0.15h\mathrm{Mpc}^{-1}$, a discrepancy that becomes more pronounced at higher wavenumbers. The other symbols show the spectra measured for samples of dark matter haloes defined by different minimum mass thresholds; the amplitude of the points increases with the mass cut. These spectra have been corrected for shot noise by subtracting $1/\bar{n}$, where $\bar{n}$ is the number density of haloes. This correction is important as the mean separation of the haloes is close to the scale of the feature we are trying to measure. The solid lines show the linear theory spectrum multiplied by the square of an effective bias computed for each sample (see Padilla & Baugh 2002). This model for the halo spectrum gives a good match to the simulation for $k \lesssim 0.07h\mathrm{Mpc}^{-1}$, but underestimates the power at higher wavenumbers. Although nonlinear evolution erases the acoustic oscillations at high k, the first few oscillations are still clearly visible in the cluster power spectrum.

The impact of peculiar motions and redshift errors is illustrated in Fig. 2. The symbols show the real-space power spectra of two halo samples. The dotted and dashed lines show fits to the halo power spectrum measured in redshift-space, with and without redshift errors respectively. (The fitting process is discussed in §3.) Redshift-space positions are

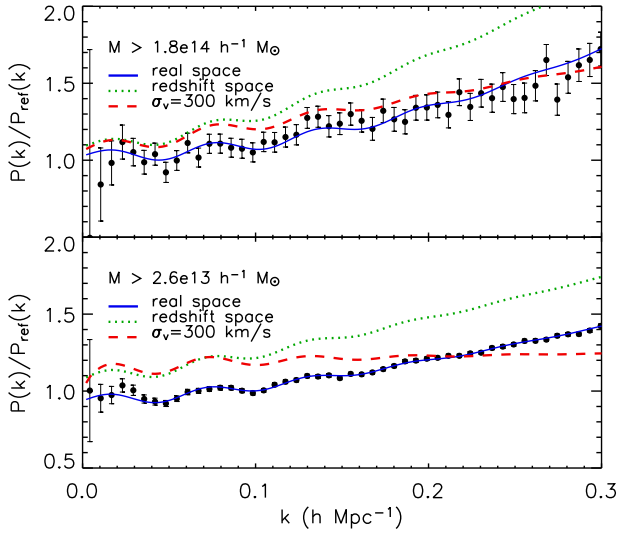

Figure 2. Fits to the power spectra of haloes. The points show the measured real-space spectrum and the lines show the best fits for three cases: real-space positions, redshift-space positions and redshift-space plus redshift measurement errors, as indicated by the legend. The panels correspond to different mass limits.

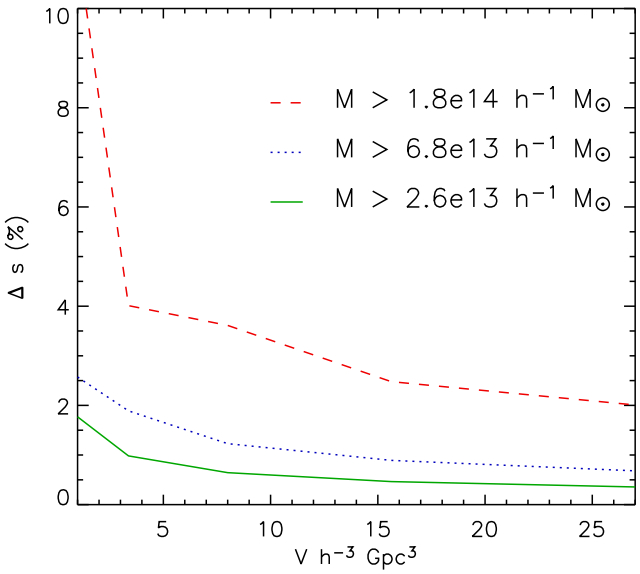

Figure 3. The percentage error in the recovered sound horizon as a function of survey volume. The lines correspond to samples with different minimum mass thresholds, as given in the legend.

calculated in the distant observer approximation by adding the scaled x component of the peculiar motion of the centre of mass to the x coordinate of each halo. For illustration, we show the impact of an error in the cluster redshift given by a Gaussian with variance 300 km s^{-1}. At low k we find a shift in the amplitude of the spectrum in redshift-space relative to real-space. The size of this shift is smaller for the larger mass sample, due to its larger effective bias.

For dark matter or galaxies, redshift-space distortions generally cause a shift in the spectrum on large scales and damping on smaller scales relative to the real-space spectrum (e.g. Benson et al. 2000). However, for clusters, the overall distortion in the power spectrum is more complicated, as noted by Padilla & Baugh (2002). Cluster-size haloes are in a rather different clustering regime from the dark matter or galaxies for three reasons. Firstly, the mean halo separation exceeds the correlation length by a factor of 2-4, depending upon mass. Secondly, haloes correspond to high peaks in the density field. Finally, haloes are not located in virialized structures; otherwise the group finder would have simply identified the supercluster as a dark matter halo of larger mass. Redshift errors depress the power spectrum at high k because they smear out structures on scales comparable to the size of the equivalent spatial error. This effect partially compensates for the redshift-space distortion, bringing the result closer to the real-space estimate. The discrepancies between the spectrum that we recover for massive haloes in redshift-space and the naive expectations based on extrapolations of linear theory or results for galaxies are a good illustration of the need to use a full N-body calculation in order to model the power spectrum correctly.

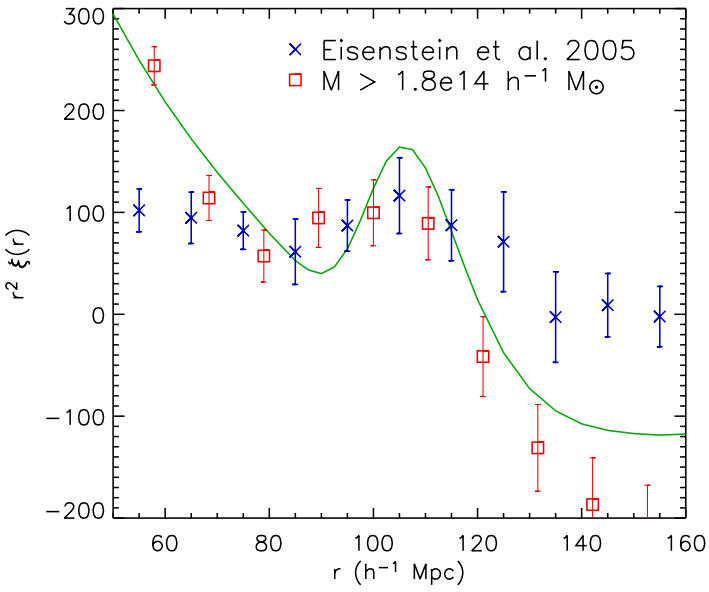

Figure 4. The correlation function, $\xi(r)$, of haloes with $M > 1.8 \times 10^{14} h^{-1} M_{\odot}$ (squares) compared with linear perturbation theory (solid line), which includes the effective bias of the haloes and redshift-space distortions. We plot $r^2\xi(r)$ to expand the dynamic range. The correlation function of luminous red galaxies is also plotted for comparison (crosses; Eisenstein et al. 2005).

3 MEASURING THE SOUND HORIZON

We take a somewhat different approach to determine the sound horizon scale to that of BG03, who fitted a parametric form to the ratio of the measured power spectrum to a reference spectrum without oscillatory features. Instead, we fit to the power spectrum directly, using the analytic matter

power spectrum presented by Eisenstein & Hu (1999), which describes the linear theory fluctuations in the cold dark matter and baryons. We model the effects of nonlinear evolution using a simple approximation, which effectively linearizes the power spectrum by removing the nonlinear distortion. We first divide both the measured spectrum and the corresponding linear theory spectrum by a smooth reference. The ratios obtained for the measured spectrum and the linear theory spectrum differ beyond a particular wavenumber, $k_{\rm nl}$ (Fig. 1). We fit a linear relation to the measured power spectrum ratio beyond $k_{\rm nl}$, $P/P_{\rm ref} = A+Bk$. We then divide the measured ratio by $A+Bk$ and multiply the result by the reference spectrum to get a linearized power spectrum. The free parameters in the linearization step are $k_{\rm nl}$, A and B. We then fit the linearized spectrum to the Eisenstein & Hu formula. The free parameters are the sound horizon scale, Ω_m, Ω_b, h and the amplitude of the spectrum. The values of Ω_m, Ω_b and h are set to those used in the simulation.

Our approach has a number of clear advantages over that of BG03. Firstly, BG03 fit to the measured spectrum divided by a reference spectrum. There is no statistical gain to be derived from this; we present our results as a ratio in Figs. 1 and 2 simply to improve the contrast of the oscillations. As a matter of fact, the choice of reference can compromise the fit as different choices for the smooth spectrum can alter the visibility of the first peak, leading to possible systematic errors in the derived sound horizon scale. Secondly, the form advocated by BG03 is an approximation based on a Taylor expansion of the combined transfer functions for cold dark matter and baryons. The parameter that BG03 equate to the sound horizon is actually only equivalent to this scale under certain conditions. Thirdly, BG03's parametric form is only applicable when fluctuations are in the linear regime. In hierarchical models, nonlinearities lead to deviations from the linear theory spectrum on surprisingly large scales (see Fig. 1 and Figure 4 of Baugh & Efstathiou 1994). Finally, by fitting to the power spectrum rather than a ratio, we are using information about the overall shape of the power spectrum, including the break, which is also sensitive to the sound horizon scale. We find that we recover a more accurate estimate of the sound horizon scale when we fit to the power spectrum directly instead of to a ratio.

The error on the spectrum depends upon the volume and the amplitude of the spectrum relative to the shot noise due to the discreteness of the tracers of the mass distribution, and is given by (Feldman, Kaiser & Peacock 1994):

$$\frac{\sigma}{P} = 2\pi\sqrt{\frac{1}{Vk^2\Delta k}}\left(\frac{1+\bar{n}P}{\bar{n}P}\right), \qquad (1)$$

where V is the survey volume, Δk is the width of the bins used to average the spectrum and $\bar{n}$ is the mean number density of clusters. All quantities are comoving. The product $\bar{n}P$ is the signal-to-noise ratio of the measured power and depends upon k. We have tested Eq. 1 against the dispersion between the spectra measured on subdividing the Hubble Volume simulation.

The fits to the power spectra measured for two samples of haloes in the full simulation are shown in Fig. 2. As explained above, we show the results after dividing by a smooth reference simply to expand the range on the y-axis. We show the best fit in three cases: the cluster power spectrum measured in real-space, in redshift-space and in redshift-space with a redshift error of $\sigma_V = 300{\rm kms}^{-1}$. Even though the shapes of the spectra are quite different, our method recovers the theoretical value of the sound horizon scale accurately. Results for three samples of haloes drawn from the full Hubble Volume simulation output at $z = 1$ are given in Table 1. The accuracy with which we predict that the sound horizon scale can be extracted from the halo power spectrum for different cubical volumes is given in Fig. 3.

Table 1. The accuracy with which the sound horizon can be measured. Column (1): The lower mass limit of the sample. (2) The number of haloes above this mass in the ΛCDM Hubble Volume output at $z = 1$. (3) The accuracy (%) with which the sound horizon is measured from the halo power spectrum. (4) The corresponding accuracy with which w is constrained.

halo mass ($h^{-1}M_\odot$)	number of haloes	Δs (%)	Δw (%)
$> 1.8\times10^{14}$	45 000	2.1	9
$> 6.8\times10^{13}$	380 000	0.7	3
$> 2.6\times10^{13}$	2000 000	0.4	1.5

The sound horizon can also be measured from the correlation function. In this case, the signature is a spike at a comoving pair separation approximately equal to the sound horizon scale. Fig. 4 shows the correlation function of haloes with a minimum mass of $1.8\times10^{14}h^{-1}M_\odot$. There is a clear peak at $\sim 105h^{-1}$Mpc. Significant differences remain between the simulations results and linear perturbation theory, even after the effective bias of the halo sample and redshift-space distortions (Kaiser 1987) are taken into account. Fig.4 also shows the correlation function of luminous red galaxies at $z \sim 0.35$ (Eisenstein et al. 2005). The correlation amplitude and errors are comparable to those of our sample of clusters at $z = 1$, which is purely a coincidence. The peak is better defined in the cluster sample, further illustrating the ability of this method to yield information on the dark energy equation of state at different redshifts.

4 DISCUSSION AND CONCLUSIONS

The dark energy equation of state can be constrained by comparing measurements of the acoustic horizon derived from the power spectrum of galaxy clusters and from temperature anisotropies in the microwave background. WMAP data constrain the sound horizon scale to an accuracy of $\sim 3\%$ (Spergel et al. 2003); this will undoubtedly improve in the future. In principle, w can be estimated from both the radial and transverse parts of the power spectrum. The acoustic horizon is a comoving standard ruler whereas cluster surveys measure redshifts and angular positions. Transforming redshifts to comoving distances requires the Hubble parameter, $H(z)$, while transforming angular separations involves the angular-diameter distance, $D_A(z)$. Both $H(z)$ and $D_A(z)$ depend on w as well as other cosmological parameters. Thus, the radial and tangential components of the spectrum provide independent routes to w. In practice, it is unlikely that realistic surveys will have sufficient spectral modes for such a decomposition, so one may have to resort to the spherically averaged power spectrum used here.

The cluster power spectrum gives a purely geometrical test for w based on absolute distances. By contrast, the

test based on distant supernovae (also geometrical) relies on relative distance measurements, while the test based on counting clusters as a function of redshift depends on a combination of geometry and the fluctuation growth rate. These tests are therefore complementary and, in principle, measure different things. The utility of the counts is limited by the accuracy with which an observation, e.g. the Sunyaev-Zeldovich (SZ) decrement, can be translated into an estimate of halo mass which is required to link with theory (Majumdar & Mohr 2003; Wang et al. 2004). Whilst the sensitivity to cluster mass can be reduced by combining the number counts with a measurement of the amplitude of the cluster power spectrum, this "self-calibration" is still model dependent (Majumdar & Mohr 2004). Our method does not require a detailed knowledge of cluster masses as these affect the amplitude but not the shape of the power spectrum.

All methods measure a weighted integral of w over redshift (Deep Saini, Padmanabhan & Bridle 2003). Recent estimates at low redshift already constrain w to $\approx 20\%$ in the simplest, $w = -1$, model (e.g. Riess et al. 2004). Measurements at $z \gtrsim 1$ are therefore of great interest. With acoustic oscillations, there is the added incentive that the measurement becomes easier at higher redshift because fewer high k oscillations have been erased by nonlinear gravitational evolution. This gain is partly offset by the greater difficulty in finding clusters at high redshift (though the SZ effect is independent of redshift). For baryon oscillations, $z \sim 1$ is a particularly interesting epoch because the dependence of the method on the parameter $\Omega_m h^2$ cancels out to first order for $w \simeq -1$ (e.g. BG03); hence the focus on $z \sim 1$. We have shown that the impact of baryons on the form of the power spectrum of cluster-mass haloes at $z \sim 1$ is clearly visible. For the idealised case of a cubical volume, it is possible, with a big enough survey, to measure the acoustic horizon to an accuracy of $\approx 2\%$. In practice, several effects such as uncertainties in the cosmological parameters and the impact of the survey geometry on the measurement of the power spectrum will need to be taken into account. Our method allows a competitive constraint, $\Delta w \approx 10\%$, on the dark energy equation of state at $z \sim 1$ (Angulo et al, in prep).

Suitable samples of clusters at $z \sim 1$ could be obtained in a variety of ways. First, a catalogue of clusters on the sky is required. This could be constructed from optical and near infrared photometry, using the red sequence of early type galaxies (Gladders & Yee 2005). The photometry could also be exploited to estimate the cluster redshift (e.g. Kodama, Bell & Bower 1999). Gladders & Yee (2005) report an accuracy of $\sigma_z \approx 0.02 - 0.03$ using two bands that straddle the $4000\mathring{A}$ break at $z \sim 1$. Large area photometric surveys are currently being proposed. For example, equipped with an optical camera, VISTA (http://www.vista.ac.uk) would be able to survey 10,000 square degrees in UVRI to $B \approx 25$ in 200 photometric nights and the Dark Energy Survey (DES, http://cosmology.astro.uiuc.edu/DES/) plans to cover 4,000 square degrees to a similar depth. Alternatively, the SZ effect could be used to identify clusters on the sky (Carlstrom, Holder & Reese 2002). The South Pole Telescope (SPT) aims to detect 40,000 SZ clusters over 4,000 square degrees at $z \sim 0.5 - 1$ (Ruhl et al. 2004). Photometric redshifts for these could be obtained with the DES which plans to cover the same area. The objects in our most massive halo sample are comparable to those that the SPT will detect at $z \sim 1$.

Our test requires cluster redshifts. Obtaining spectroscopy for thousands of clusters is not trivial. With AAΩ, the new multi-object spectrograph at the Anglo Australian Observatory, a redshift for a bright early type galaxy at $z \sim 1$ can be obtained in 100-200 minutes. There are typically 30 clusters per field of view, so a survey of 40,000 clusters would need ≈ 200 clear nights; an equivalent spectrograph on an 8m telescope would reduce this to 50 nights. Photometric redshifts are an alternative but the reduced accuracy leads to a serious loss of information (Blake & Bridle 2005). The error in the cluster redshift causes a damping of the power at $k_x > 1/\sigma_x$, where σ_x is the scaled error in the comoving cluster position. For the photometric redshift accuracy reported by Gladders & Yee (2005), $\sigma_x \approx 140 h^{-1}$Mpc at $z = 1$. The damping of the spectrum can be circumvented if modes with $k_x > 1/\sigma_x$ are discarded, thus effectively using the full spectrum at $k_x < 1/\sigma_x$ and the transverse spectrum for $k_x > 1/\sigma$. The associated reduction in the number of k-modes (by a factor of ~ 20; see Blake & Bridle 2005) could be compensated for in several ways: (i) Increasing the solid angle covered. (ii) Improving the photometric redshift estimate by using more filters and deeper photometry. (iii) Using a lower mass to define the halo sample. Although further exploration of this idea using a mock catalogue of a specific survey is needed, our idealized calculation suggests that this is a powerful method for obtaining interesting constraints on the properties of the dark energy.

ACKNOWLEDGEMENTS

This work was supported by the EC's ALFA scheme via funding the Latin American European Network for Astrophysics and Cosmology and by PPARC; CMB is supported by the Royal Society. We acknowledge discussions with Chris Blake, Sarah Bridle, Francisco Castander, Enrique Gaztañaga and Mike Gladders.

REFERENCES

Abazajian K., et al. 2004, AJ, 128, 502
Bardeen J., Bond J. R., Kaiser N., Szalay A., 1986, ApJ, 304, 15
Baugh C. M., Efstathiou G., 1994, MNRAS, 270, 183
Benson A. J., et al., 2000, MNRAS, 316, 107
Bower R.G., Coles P., et al., 1993, ApJ, 405, 403
Blake C., Glazebrook K., 2003, ApJ, 594, 665. (BG03)
Blake C., Bridle S., 2005, (astro-ph/0411713)
Carlstrom J. E., Holder G., Reese E. D., 2002, ARAA, 40, 643
Colberg J. M., et al., 2000, MNRAS, 319, 209
Cole S., Hatton S., et al., 1998, MNRAS, 300, 945
Cole S., et al., 2005, MNRAS, submitted. (astro-ph/0501174)
de Bernardis P., et al. 2000, Nature, 404, 955
Deep Saini, T., et al., 2003, MNRAS 343, 533
Davis M., Efstathiou G., et al., 1985, ApJ, 292, 371
Efstathiou G., et al., 2002, MNRAS, 330, L29
Eisenstein D. J., Hu W. 1999, ApJ, 511, 5
Eisenstein D. J., Hu W., Tegmark M., 1998, ApJ, 504, 57
Eisenstein D. J., et al., 2005, ApJ, submitted. (astro-ph/0501171)
Evrard A. E., et al., 2002, ApJ, 573, 7
Feldman H. A., Kaiser N., Peacock J. A. 1994, ApJ, 426, 23
Gladders M. D., Yee H. K. C., 2005, ApJS, 157, 1
Hu W., Haiman Z., 2003, Phys. Rev. D., 68, 3004
Jenkins A., et al., 2001, MNRAS, 321, 372
Kaiser N., 1984, ApJ, 284, L9
Kaiser N., 1987, MNRAS, 227, 1
Kodama T., Bell E. F., Bower R. G., 1999, MNRAS, 302, 152
Linder E. V., 2003, PhRvD, 68, 3503
Majumdar S., Mohr J. J., 2003, ApJ, 585, 603

Majumdar S., Mohr J. J., 2004, ApJ, 613, 41
Meiskin A., White M., Peacock J. A. 1999, MNRAS, 304, 851
Narayanan V.K., Berlind A., Weinberg D., 2000, ApJ, 528, 1
Padilla N. D., Baugh C. M., 2002, MNRAS, 329, 431
Padilla N. D., et al., 2004, MNRAS, 352, 211
Peacock J. A., et al., 2001, Nature, 410, 169
Percival W. J., et al., 2001, MNRAS, 327, 1297
Percival W. J., et al., 2002, MNRAS, 337, 1068
Perlmutter S. et al., 1999, ApJ, 517, 565
Riess A. G., et al., 1998, AJ, 116, 1009
Riess A. G., et al., 2004, ApJ, 607, 665
Ruhl J., et al., 2004, SPIE, 5498, 11
Seo H., Eisenstein D. J., 2003, ApJ, 598, 720
Spergel D. N., et al., 2003, ApJS, 148, 175
Springel V., et al., 2005, Nature, 435, 439
Tegmark M., et al. 2004, PhRvD, 69, 103501
Wang S., et al., 2004, PhyRvD, 70, 123008